

## Probing the collective Josephson plasma resonance in $\text{Bi}_2\text{Sr}_2\text{CaCu}_2\text{O}_{8+y}$ by $W$ -band-mixing experiments

W. Walkenhorst, G. Hechtfischer, S. Schlötzer, R. Kleiner, and P. Müller  
*Physikalisches Institut III, Universität Erlangen-Nürnberg, D-91058 Erlangen, Germany*  
 (Received 25 April 1997)

We report on  $W$ -band-mixing experiments with mesa structures patterned on top of  $\text{Bi}_2\text{Sr}_2\text{CaCu}_2\text{O}_{8+y}$  single crystals. Due to the intrinsic Josephson effect the mixing process could be observed. There is a steep increase of the mixing intensity when the bias current approaches the critical current. We show that the mixing response is related to the excitation of the collective Josephson plasma resonance. In magnetic fields we observed a decrease of the Josephson plasma frequency. From this dependence we were able to estimate the frequency of the Josephson plasma resonance for zero bias and zero field ranging from 105 to 220 GHz. [S0163-1829(97)06837-9]

### I. INTRODUCTION

Due to their large gap voltages high-temperature superconductors are promising candidates for high-frequency applications in the THz regime.<sup>1</sup> Therefore, it is highly desirable to study high-frequency properties and especially collective behavior of oscillating charges. In a single Josephson junction the collective oscillation of Cooper pairs has been predicted by Josephson<sup>2</sup> and was found experimentally by Dahm *et al.*<sup>3</sup> in a point contact. This collective mode is known as Josephson plasma resonance. The intrinsic Josephson effect in  $\text{Bi}_2\text{Sr}_2\text{CaCu}_2\text{O}_{8+y}$  provides closely packed Josephson junctions.<sup>4</sup> Therefore, the Cooper-pairs are supposed to oscillate not only across one single junction but coherence should extend over the whole stack. In layered Josephson junctions this collective mode has been predicted by Tachiki *et al.*<sup>5</sup> and is responsible for the magnetoabsorption resonance observed in  $\text{Bi}_2\text{Sr}_2\text{CaCu}_2\text{O}_{8+y}$  single crystals in the frequency range of 30–60 GHz.<sup>6–8</sup> In these experiments relatively large crystals (0.5 mm in  $a$ - $b$  direction) are irradiated with a microwave field with the  $E$ -field vector perpendicular to the  $\text{CuO}_2$  layers. In addition, a static magnetic field  $H$  was applied along the crystallographic  $c$ -axis. For  $H=0$  the frequency of the plasma resonance  $f_{\text{pl}}$  is well above 100 GHz and thus outside of the detection window. The effect of the magnetic field is to lower  $f_{\text{pl}}$  by reducing the  $c$ -axis critical current density of the sample and thereby decreasing the plasma resonance. The surface resistance of the crystals strongly increases when the frequency  $f_{\text{pl}}$  of the Josephson plasma resonance matches the external frequency. Although these experiments yielded good evidence for the existence of the collective Josephson plasma resonance we intended to investigate this resonance in zero magnetic field. In order to apply a bias current we use systems of well defined geometry, i.e., small-sized stacks of Josephson junctions on top of single crystals (mesas). We intend to test whether the collective plasma resonance can be detuned by a bias current and can be used for high-frequency applications. Moreover, we want to investigate to what extent the collective Josephson plasma mode is similar or different from what is known from the plasma resonance in classic single junctions.

We performed mixing experiments by applying two external microwave signals of approximately 90 GHz to small-sized mesas on top of  $\text{Bi}_2\text{Sr}_2\text{CaCu}_2\text{O}_{8+y}$  single crystals. The mesas form stacks of typically 100 intrinsic Josephson junctions.<sup>4,9</sup> The intensity of the incident microwave fields was converted down to the difference frequency of the applied signals by using the sample as mixing element. We will show that this method is advantageous in order to separate nontrivial effects arising simply from impedance mismatch. Applying a single microwave signal yields information about absorption or reflection only and impedance effects can be on the same order as the investigated effects. In mixing experiments, impedance effects are still present but can be distinguished from the mixing process by additional reflection measurements. We will show that the interaction of the two microwave fields with the plasma resonance leads to an enhanced mixing signal. This allows to investigate the plasma resonance and its dependence on bias current and magnetic field.

In the following we will first motivate the interaction between the Josephson plasma resonance and two external microwave fields in the context of the resistively shunted junction (RSJ) model and will then turn to experimental results.

### II. MIXING IN THE CONTEXT OF THE RSJ MODEL

A simple theoretical approach to real Josephson junctions in the limit of short single junctions is given by the RSJ model.<sup>10</sup> Here, the current through the junction is described as a sum of the ideal Josephson current given by the first Josephson equation, an ohmic quasiparticle current, and a displacement current due to the nonzero junction capacitance. Substituting the voltage drop over the junction barrier via the second Josephson equation yields the RSJ equation

$$I = I_c \sin \gamma + \frac{\hbar}{2eR_n} \dot{\gamma} + \frac{\hbar C}{2e} \ddot{\gamma}, \quad (1)$$

where  $I$  is the external current,  $I_c$  the maximum Josephson current,  $\gamma$  the phase difference across the junction barrier,  $C$

the junction capacitance and  $R_n$  the normal resistance. The eigenresonance at zero bias current, the Josephson plasma resonance, is given by

$$f_{\text{pl},0} = \frac{\omega_{\text{pl},0}}{2\pi} = \sqrt{\frac{j_c d}{2\pi\Phi_0\epsilon_0\epsilon_r}}, \quad (2)$$

where  $\Phi_0 = h/2e$  denotes the flux quantum,  $j_c$  is the critical current density, and  $d$  is the interlayer distance. Therefore, for realistic values of  $j_c = 800 \text{ A/cm}^2$  and a dielectric constant  $\epsilon_r = 5$  one would expect  $f_{\text{pl}}$  to be of the order of 150 GHz. With  $\epsilon_r = 1$  one obtains an upper limit for the Josephson plasma resonance of 320 GHz. In the RSJ model the Josephson plasma resonance of a single Josephson junction decreases with bias current according to<sup>11</sup>

$$f_{\text{pl}} = f_{\text{pl},0} \sqrt{1 - \left(\frac{I_b}{I_c}\right)^2}, \quad (3)$$

where  $I_b$  is dc bias current. The external current  $I$  in the presence of two external microwave fields of frequencies  $f_1$  and  $f_2$  is

$$I = I_b + I_{\text{ac}1} \cos(2\pi f_1 t) + I_{\text{ac}2} \cos(2\pi f_2 t). \quad (4)$$

$I_{\text{ac}1}$  and  $I_{\text{ac}2}$  denote the amplitudes of the ac currents coupled to the junction by the two microwave fields. We assume  $I_{\text{ac}1}, I_{\text{ac}2} \ll I_c$ , and  $|f_1 - f_2| \ll f_1, f_2 < f_{\text{pl},0}$ . For simplicity, we neglect the damping term in Eq. (1). Approximating the time dependent phase difference as

$$\begin{aligned} \gamma &\approx \gamma_0 + \gamma_1 \cos(2\pi f_1 t) + \gamma_2 \cos(2\pi f_2 t) \\ &\quad + \gamma_{\text{mix}} \cos[2\pi(f_1 - f_2)t] \\ &=: \gamma_0 + \epsilon \end{aligned} \quad (5)$$

( $\gamma_1, \gamma_2$  are the amplitudes of the induced phase differences and  $\gamma_{\text{mix}}$  is the amplitude of the resulting phase difference with the difference frequency) and expanding  $\sin \gamma$  for  $\epsilon \ll \gamma_0$  up to second order,

$$\sin \gamma \approx \sin \gamma_0 + \epsilon \cos \gamma_0 - 1/2 \epsilon^2 \sin \gamma_0 \quad (6)$$

we get from Eq. (1) for the amplitude of the mixing product

$$\gamma_{\text{mix}} \propto \frac{I_b I_{\text{ac}1} I_{\text{ac}2}}{(f_{\text{pl}}^2 - f_1^2)(f_{\text{pl}}^2 - f_2^2)}. \quad (7)$$

It diverges when either  $f_1$  or  $f_2$  are equal to  $f_{\text{pl}}$ . Note that these divergencies result due to the neglected damping term in Eq. (1). Otherwise,  $\gamma_{\text{mix}}$  would be large but finite. According to Eq. (7), strong frequency conversion should be expected when the external frequencies match the Josephson plasma resonance. Note that applying only one single external microwave signal does not lead to mixing because of  $I_{\text{ac}2} = 0$  and therefore  $\gamma_{\text{mix}} = 0$ . Especially, there is no Josephson plasma self-mixing.

An alternative way to derive the influence of the plasma resonance on mixing is a description in terms of a nonlinear inductance  $L(I)$ , as discussed in the context of parametric amplification.<sup>12</sup> Strong mixing occurs when  $\partial L / \partial I$  is large.<sup>13</sup> By comparing the identities

$$U = \frac{\hbar}{2e} \frac{\partial}{\partial t} \gamma \quad \text{and} \quad U = \frac{\partial}{\partial t} (LI) \quad (8)$$

one obtains an expression for the Josephson inductance:

$$L = \frac{\hbar}{2eI} \gamma. \quad (9)$$

To answer the question how this inductance behaves under irradiation we consider only one external microwave signal with frequency  $f_{\text{ext}}$  for  $I \neq 0$ . Again, treating the microwave signal as a small quantity we find from Eq. (1)

$$\gamma \approx \gamma_0 + \frac{I_{\text{ac}}}{I_c} \frac{f_{\text{pl},0}^2}{f_{\text{pl}}^2 - f_{\text{ext}}^2} \cos(2\pi f_{\text{ext}} t), \quad (10)$$

with  $\gamma_0 = \arcsin(I_b/I_c)$ . We thus get

$$L = \frac{\hbar}{2eI} \left[ \frac{I_{\text{ac}} \cos(2\pi f_{\text{ext}} t)}{I_c} \frac{f_{\text{pl},0}^2}{f_{\text{pl}}^2 - f_{\text{ext}}^2} + \gamma_0 \right], \quad (11)$$

and derive

$$\frac{\partial L}{\partial I} = -\frac{L}{I} + \frac{\hbar}{2eI_c I} \left[ \frac{f_{\text{pl},0}^2}{f_{\text{pl}}^2} + \frac{I_b(I - I_b)}{I_c^2} \frac{f_{\text{pl},0}^6}{f_{\text{pl}}^2(f_{\text{pl}}^2 - f_{\text{ext}}^2)} \right]. \quad (12)$$

This expression peaks either when  $f_{\text{pl}} = 0$ , that is,  $I_b = I_c$ , or when the plasma resonance matches the external frequency. To summarize the results, applying two external signals leads to mixing due to terms in  $\gamma^2$ . The more technical reason for the appearance of mixing signals is the strong increase of the nonlinearity in the Josephson inductance. In our case we use a nonlinear reactance instead of a nonlinear resistance which is used in standard mixing processes.

So far, our analysis has been based on some approximations. In order to confirm these results we also performed numerical simulations of Eq. (1). Here, we trace the time dependence of the voltage across the junction. After Fourier transformation we obtain the frequency spectrum. We then calculate the intensity in the mixing channel as function of bias current. We consider the situation shown in Fig. 1(a). As a function of bias current the plasma frequency varies according to Eq. (3). At a certain value of  $I_b$ ,  $f_{\text{pl}}$  matches the external frequencies  $f_1 = f_{\text{LO}}$  and  $f_2 = f_{\text{RF}}$ . LO denotes the local oscillator and RF the radio frequency signal, respectively.

We consider a situation where  $f_{\text{LO}}/f_{\text{pl},0} = 0.87$  and  $f_{\text{RF}}/f_{\text{pl},0} = 0.74$ . The amplitudes of the signals are  $I_{\text{LO}}/I_c = 0.01$  and  $I_{\text{RF}}/I_c = 0.001$ , respectively. The numerically calculated response is shown in Fig. 1(b). There are two distinct maxima when the plasma resonance matches the frequency of the applied signals. Figure 1(c) shows a simulation with lower values of  $f_{\text{LO}}/f_{\text{pl},0} = 0.67$  and  $f_{\text{RF}}/f_{\text{pl},0} = 0.54$ . As expected, the conversion peaks shift closer to the critical current.

The difference in the height of the two peaks is caused by the bias current dependence of  $L$ . Even in absence of external microwave fields the nonlinearity in  $L$  increases while approaching the critical current. We also confirmed that the mixing signal disappeared when the amplitude of either the LO or the RF signal was set to zero. In the simulations

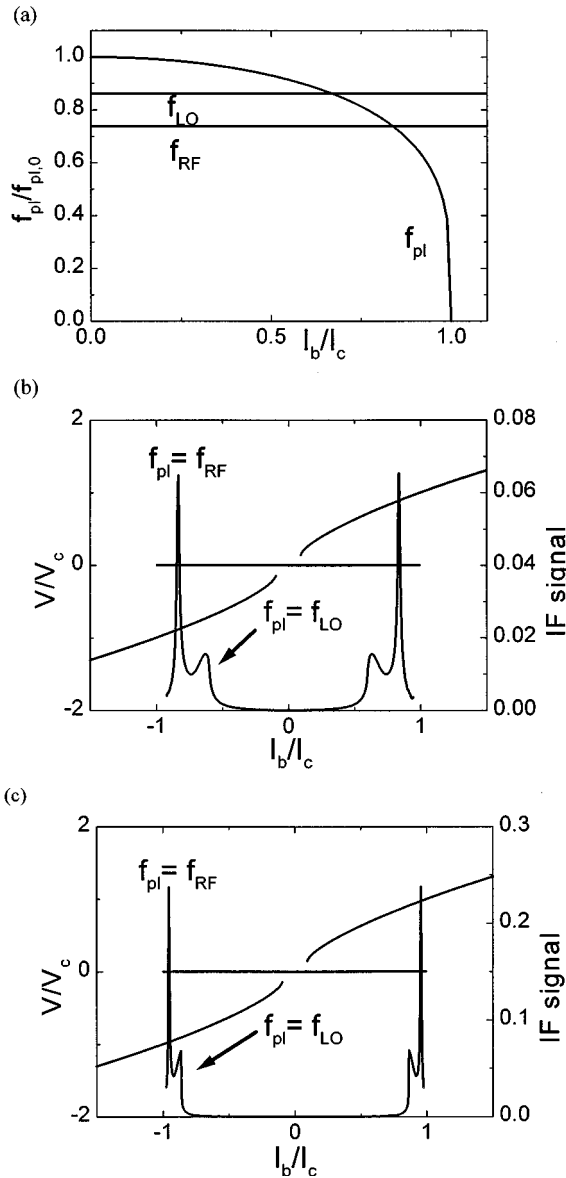


FIG. 1. RSJ simulations. (a) Plasma frequency, RF, and LO frequency as a function of bias current normalized to the critical current  $I_c$ . The ratio of  $f_{LO}/f_{pl,0}=0.87$ ;  $f_{RF}/f_{pl,0}=0.74$ . (b) Mixing response as function of bias current.  $f_{LO}/f_{pl,0}$  and  $f_{RF}/f_{pl,0}$  are as in (a). (c) Mixing response for  $f_{LO}/f_{pl,0}=0.67$  and  $f_{RF}/f_{pl,0}=0.54$ . Conversion peaks move closer to  $I_c$ .

shown in Fig. 1 the conversion peaks are at the positions where the frequency of the plasma resonance matches the frequencies of the external signals. For higher LO amplitudes the peaks shifted significantly towards lower bias currents. Therefore, in our mixing experiments we kept LO and RF signal as small as possible. We finally note that in our experiments  $f_{RF}$  and  $f_{LO}$  are about 90 GHz differing by less than 5 GHz. From the experiments of Refs. 6–8,14,15 and the above estimation we expect the Josephson plasma frequency  $f_{pl}$  to be 150 GHz or larger. In addition, we expect a broadening of the plasma resonance due to dissipation mechanisms.<sup>16</sup> Thus, the two conversion peaks should essentially collapse to a single peak which is located very close to the critical current. Then, because of noise and instabilities due to the excited plasma resonance the junction might

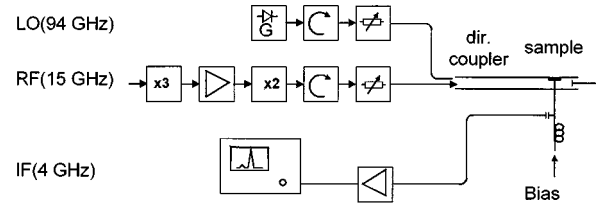


FIG. 2. Setup. A tunable Gunn diode acts as local oscillator. The RF signal is a multiplied 15 GHz signal. Both, local oscillator radiation and RF signal can be variably attenuated. They are led via a directional coupler and a waveguide to the sample mounted in a resonator. The intermediate frequency is amplified and then detected by a spectrum analyzer. The coupling to the sample could be adjusted by a variable short.

switch to its resistive state, even slightly below the critical current. These noise phenomena are not taken into account in the simulations. They would have been too time consuming.

### III. SAMPLES AND MEASUREMENT TECHNIQUE

Single crystals of  $\text{Bi}_2\text{Sr}_2\text{CaCu}_2\text{O}_{8+y}$  were grown from a stoichiometric mixture of the oxides.<sup>4</sup> Using chemical wet etching, mesas with lateral dimensions varying from  $16 \times 16 \mu\text{m}^2$  to  $28 \times 28 \mu\text{m}^2$  were patterned on top of single crystal surfaces. Mesa heights varied from 18 to 200 nm corresponding to 12–150 intrinsic Josephson junctions. As the electrical contact, a gold layer was evaporated onto the freshly cleaved top surface of the mesa and a  $25 \mu\text{m}$  Au/Ni wire was used as a spring contact to the gold layer. Transport measurements were performed in two-point geometry. Critical temperatures of the samples ranged between 85 and 89 K, and critical current densities at 4.2 K were  $312 \text{ A/cm}^2$  to  $1.9 \text{ kA/cm}^2$ . The characteristic voltages  $V_c = I_c R_n$  of the samples were typically 20 mV, corresponding to a characteristic frequency of 10 THz. Samples were mounted in a W-band waveguide mixer block.<sup>17</sup> A tunable phase-locked Gunn oscillator (93–95 GHz) was used as local oscillator.<sup>18,19</sup> LO power was up to 17 dBm. The RF signal was generated by a times six multiplier chain from a frequency locked synthesizer. Maximum signal power was up to 10 dBm. Both the LO and RF signal were continuously attenuable and the coupling to the sample could be tuned by an adjustable short. The intermediate frequency (IF) was detected by a low noise amplifier in the range of 3.7 to 4.2 GHz and then supplied to a spectrum analyzer (Fig. 2). The whole setup was placed in a shielded room. Magnetic field parallel to the layers was applied via a superconducting 50 kOe solenoid. Magnetic field with variable orientations could be applied via a 8 kOe Helmholtz pair. Measurements were taken in the temperature range from 4.2 to 90 K.

We have measured the mixing response of 29 mesas on top of 24 different crystals. These crystals were prepared from 8 different melts. One of the samples (No. LJ9) was prepared at another institute.<sup>20</sup> All samples under test showed clearly the mixing behavior at zero field conditions.

### IV. MIXING RESPONSE

Figure 3(a) shows the IF spectrum of our samples. At the difference frequency  $f_{LO} - f_{RF}$  a peak was observed. Chang-

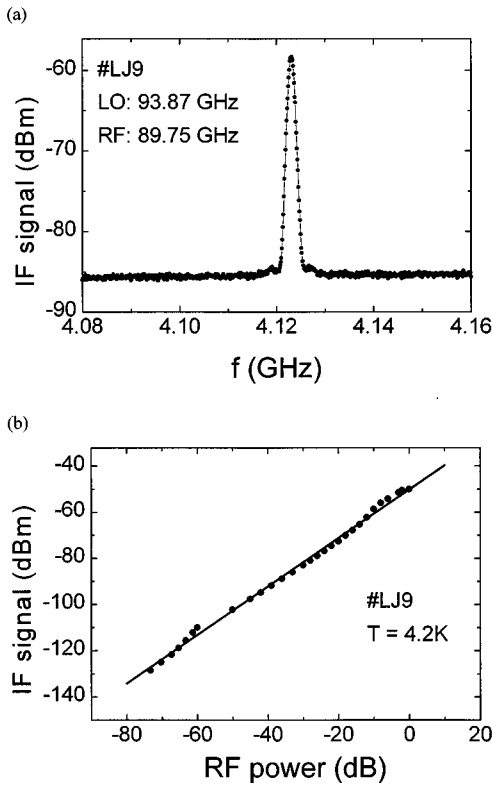


FIG. 3. Spectrum of intermediate frequency. (b) IF signal vs RF power at fixed LO power, zero magnetic field, and fixed bias current of  $600 \mu\text{A}$ . Note the constant conversion over eight orders of magnitude in RF power.

ing either  $f_{\text{LO}}$  or  $f_{\text{RF}}$  resulted in a frequency shift of the intermediate frequency channel according to  $f_{\text{LO}} - f_{\text{RF}}$ . For fixed LO power we measured the IF intensity as function of RF power [Fig. 3(b)]. We obtained constant conversion over eight orders of magnitude in applied RF power. The mixing signal intensity at fixed signal power increased with LO power until it saturates at about 5 dBm. Because of impedance mismatch there is a coupling loss of 38 dB. The required LO power for optimum mixing conversion in the sample therefore calculates to  $-33$  dBm. This number can compete with well-established quasiparticle mixers<sup>21</sup> and is much lower than required for Schottky mixers.<sup>22</sup> The conversion loss and the mixer noise figure were estimated by measuring the RF power for which the intensity of the IF signal was 3 dB over noise level. The conversion loss was estimated to 28 dB while the mixer noise figure yielded 20 dB.<sup>18,19</sup>

## V. EXPERIMENTS AT ZERO MAGNETIC FIELD

The Josephson plasma frequency at zero bias  $f_{\text{pl},0}$  should be at about 150 GHz, thus being 50% above the applied frequencies. The difference frequency is about 2% of  $f_{\text{pl},0}$ . Therefore,  $f_{\text{pl}}$  should match the applied frequencies relatively close to the critical current and we expect one broadened peak only (see Sec. II). In Fig. 4 we plot the  $IV$  characteristic (IVC) of the sample at 4.2 K (upper part) together with the intensity of the mixing signal (lower part). Ramping up the bias current  $I_b$  from zero, the maximum Josephson

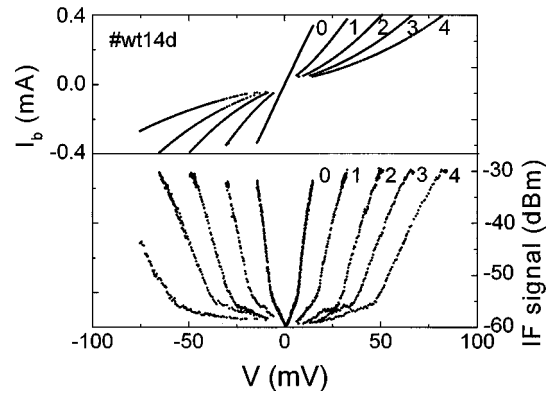


FIG. 4.  $IV$  characteristic (upper part) and IF intensity at 4.2 K and zero magnetic field (lower part). Constant resistance is not subtracted. On every branch—even on the superconducting one (denoted 0)—mixing conversion showed a steep uprise towards  $I_{c1}^*$ . Additional voltage drop is due to two point measurement. The indices denote the number of junctions in the resistive state.

current  $I_{c1}^*$  of the weakest intrinsic junction was reached at 0.35 mA. This maximum interlayer current is smaller than the critical current  $I_{c1}$  because of ac currents coupled in by the LO. Note that the linear resistance on this superconducting branch of the IVC (denoted 0) is due to contact resistance. On this superconducting branch we observed a steep rise of the conversion just below  $I_{c1}^*$ . At low currents there appeared a plateau in mixing signal. This weak structure saturated at much lower LO powers. The origin of this additional feature is still unclear.

When increasing  $I_b$  beyond  $I_{c1}^*$  the first junction of the stack switched to its quasiparticle branch. We could trace out this first resistive branch denoted 1 in Fig. 4 by lowering  $I_b$ . Note that this branch corresponds to a state where one junction of the stack is resistive, whereas all others are still in their superconducting state. On this branch we again observed an increase in mixing conversion while approaching  $I_{c2}^*$ , where the second junction switched to the resistive state. By repeatedly ramping up  $I_b$  we could trace out a total of  $N$  branches, with  $N$  being the number of junctions in the stack. This structure of the IVC is typical for intrinsic Josephson junctions.<sup>4</sup> On each branch we could detect the same mixing behavior. Plotting the mixing intensity vs bias current (Fig. 5) we verify that the distinct branches of the mixing signal coincide. Therefore, it is sufficient to detect the mixing signal as function of bias current only.

As expected the measured conversion steeply rose up to  $I_{cn}^*$  ( $I_{cn}^*$  is the maximum Josephson current of the  $n$ th junction) but did not exhibit a peak. Even small fluctuations caused the junction to switch to its resistive state before the peak is traced out completely. We investigated the conversion structures with various levels of applied microwave power. Further reduction did not change the observed structures. In particular, the conversion maximum at  $I_{cn}^*$  did not turn into a peak.

We first note that the observed mixing is not due to mixing processes such as Josephson mixing or quasiparticle mixing close to microwave induced steps. In both cases steps should arise on the IVC at voltages  $hf/2e$  and  $hf/e$ ,

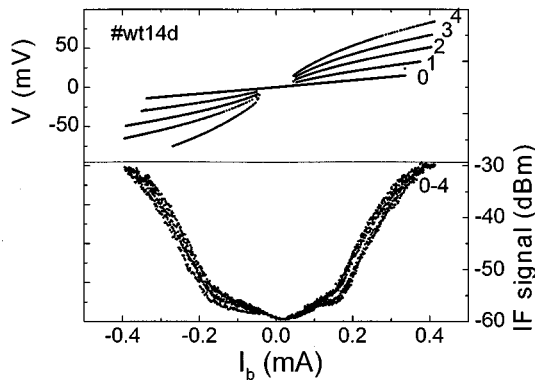


FIG. 5. Data of Fig. 4 plotted vs bias current. The mixing signals of the different branches coincide indicating that the conversion is a function of bias current only.

respectively.<sup>23</sup> We could neither detect such steps nor did we find any indication of a  $hf/2e$  or  $hf/e$  periodicity. Also, for underdamped junctions, these structures should be expected for applied frequencies well above the Josephson plasma resonance,<sup>24</sup> while we worked in the regime below it.

The observed signal cannot be simply due to mixing on a nonlinear resistance: the signal even appeared with all junctions being in the superconducting state. Here, the IVC in fact is linear (the contact resistance). Although, the resistive branches are nonlinear the mixing signal did not appear at the bias point of strongest curvature. Instead, maximum mixing occurred close to the maximum Josephson current  $I_{c1}^*$ , where the IVC is again almost linear.

Since the mixing conversion is essentially a function of bias current and is related to the superconducting state we argue that it indeed is due to the excitation of the Josephson plasma resonance. The strongest signal appeared when all junctions are in their superconducting state and the bias current approached the critical current  $I_{c1}^*$ . In states where  $n$  junctions have switched to the gap voltage only  $N-n$  junctions contribute to the conversion and IF intensity is lower. For  $n \ll N$  this resulted in a minor decrease of the intensity when increasing  $n$ . Thus, when plotting conversion vs bias current for  $n \ll N$  all conversion branches should basically

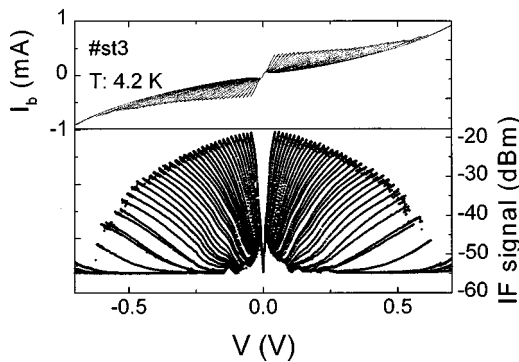


FIG. 6. IV characteristic (upper part) and IF intensity of all junctions in a whole mesa (lower part). Mixing behavior is similar on every branch. For higher order branches the conversion decreases strongly due to increasing impedance mismatch and less junctions in the superconducting state.

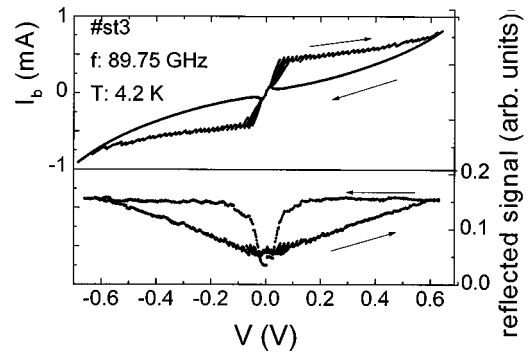


FIG. 7. IV characteristic (upper part) and reflection at 89.75 GHz (lower part). The reflected power increases with the number of junctions in the resistive state. Reflection is constant on a given branch.

coincide which is nicely confirmed by Fig. 5.

The conversion signal decreased roughly proportional to  $N-n$ . Figure 6 shows an example of the overall IVC together with the IF signal on all branches. The structure of the conversion is qualitatively the same on all branches, however, the amplitude tends to zero when approaching the  $N$ th branch. Besides the contribution of less junctions to the mixing process we ascribe this strong decrease to impedance mismatch. The impedance of the resonator structure was  $118 \Omega$  which is comparable with the mesa resistance biased on the third branch. In order to trace out effects of impedance mismatch we applied a single microwave field of 89.75 GHz and measured the reflected signal (Fig. 7). Starting from zero bias current the reflected signal increased proportional to the number of junctions in the resistive state. When decreasing the bias current again on a given branch of the IVC (Fig. 7 shows branch No. 33) the reflection remains about constant.

We thus see that impedance effects can well explain the strong decrease of the conversion on large branch numbers but has no influence on structures observed on a particular branch.

We now turn to the temperature dependence of the conversion. Figure 8 shows IVC and conversion of sample No. wt14d at  $T=80$  K. With increasing temperature the hysteresis in the IVC decreases strongly. On the other hand the

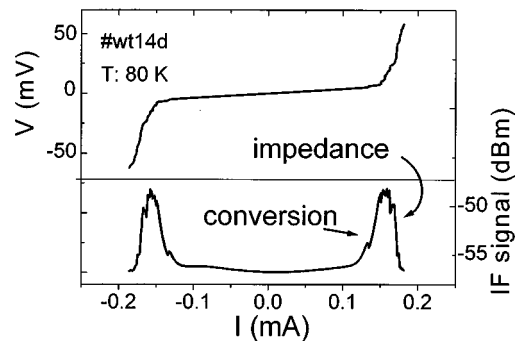


FIG. 8. IV characteristic (upper part) and IF signal at  $T=80$  K (lower part). The hysteresis of the IV characteristic decreased strongly. The mixing signal peaks below the critical current of the mesa.

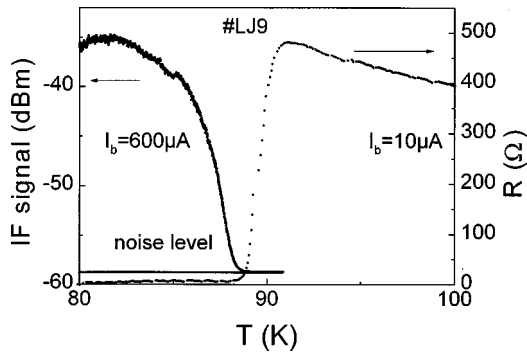


FIG. 9. Temperature dependence of sample resistance (right hand scale) and IF signal (left scale). Mixing conversion drops down to noise level when reaching the transition temperature.

critical current was almost constant up to  $T=50$  K. As long as a hysteresis can be observed the conversion on a given branch remains qualitatively the same. In terms of our interpretation this may not be unexpected since the plasma resonance is proportional to  $I_c^{-1/2}$  and thus should not change strongly. At temperatures close to  $T_c$  the IVC is nonhysteretic and the critical current decreases strongly with increasing temperature. Maximum conversion still occurs just below  $I_{cn}^*$ . The strong decrease of IF intensity above  $I_{cn}^*$  is due to increasing impedance. When heating up to the critical temperature the tends to zero. This behavior is shown in Fig. 9 where we plot the mixing signal as a function of temperature. For comparison, the figure also shows the sample resistance vs temperature. The IF signal dropped to zero exactly when nonzero resistance appears. We thus clearly see that conversion is a result of the superconducting state. Since the mixing conversion is essentially a function of bias current and is related to the superconducting state we conclude that the mixing process is due to the excitation of the Josephson plasma resonance. When almost all junctions in the stack are in their superconducting state the conversion is independent of the actual number of junctions in the resistive state. Therefore, it is even the *collective* Josephson plasma resonance causing the mixing process.

In order to investigate further properties of the resonance, we have to introduce an additional parameter. In our experi-

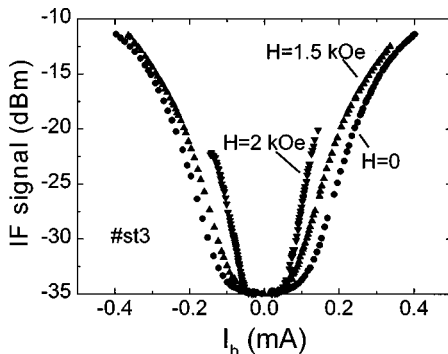


FIG. 10. IF intensity for magnetic field perpendicular to the layers. The maximum Josephson current decreased and the conversion still reached its maximum at  $I_c^*$ . Note that the mixing signals did not coincide, i.e., they are not simply ‘cut’ by the reduced  $I_c^*$ .

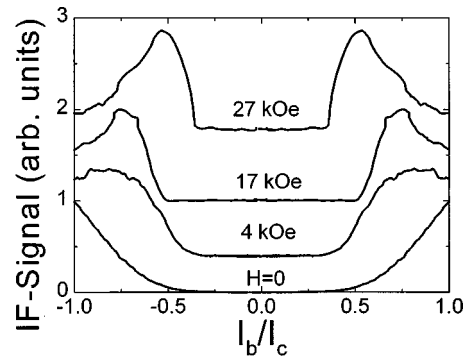


FIG. 11. IF intensity of sample No. wt15a for magnetic field parallel to the layers. The current is normalized to  $I_c(H_{\parallel})$ . Above a threshold field of about 4 kOe we detected fully developed peaks in mixing conversion vs bias current. The mixing signals are shifted for clarity. The intensities are normalized.

ments, we decided to apply a magnetic field to influence the resonance. So far, we have discussed our data in the framework of the RSJ model where effects of external magnetic fields are not covered. A more elaborate description of stacked Josephson junctions is given by coupled Sine-Gordon equations.<sup>25</sup> From these equations a set of Josephson plasma modes has been predicted<sup>26</sup> that involves nonzero  $k$  vectors both along and perpendicular to the junctions.

## VI. INFLUENCE OF MAGNETIC FIELDS

We now turn to effects of external magnetic fields. There are several effects to be expected. First of all, the influence of a magnetic field on the plasma frequency depends on field orientation. A magnetic field oriented perpendicular to the layers decreases the plasma frequency according to a power law with the exponent in the order of unity.<sup>27</sup> Applying a magnetic field parallel to the layers and perfectly aligning it should increase the resonance frequency.<sup>28</sup> Indeed, Matsuda *et al.*<sup>29</sup> could not find any magnetoabsorption resonance, when the magnetic field was aligned better than  $0.2^\circ$  parallel to the  $\text{CuO}_2$  planes of an underdoped sample. For higher tilt angles they detected plasma resonances having shifted towards lower frequencies. In our experiments we were not able to align the magnetic field that perfect. Therefore, we

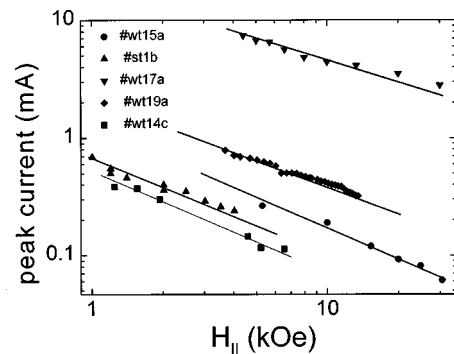


FIG. 12. Peak currents as function of  $H_{\parallel}$ . The exponents of the power laws range between 0.57 and 0.86.

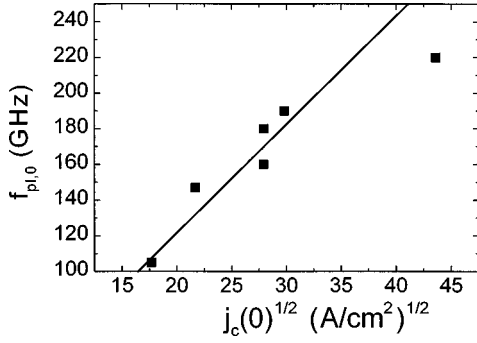


FIG. 13. Extrapolated frequencies of the Josephson plasma resonance at zero bias and zero magnetic field as function of critical current density  $j_c(H=0)$ . The line is Eq. (2) with  $\epsilon_r=3.5$ .

expect in any case a decrease of the Josephson plasma resonance with increasing field.

#### A. Magnetic field perpendicular to the $\text{CuO}_2$ layers

The main effect of magnetic fields oriented perpendicular to the  $\text{CuO}_2$  layers is to lower the frequency of the Josephson plasma resonance. According to Bulaevskii *et al.*<sup>27,28</sup> the plasma resonance should shift as

$$f_{\text{pl}}(H_{\perp}) = f_{\text{pl},0} \sqrt{\frac{I_c(H_{\perp})}{I_c(0)}}, \quad (13)$$

where  $H_{\perp}$  is magnetic field perpendicular to the  $\text{CuO}_2$  planes. This effect has been studied in the magnetoabsorption measurements.<sup>6–8</sup> From these measurements  $f_{\text{pl}}^2$  is found to decrease with magnetic field as  $H_{\perp}^{-\mu}$ , with  $\mu$  on the order of unity.<sup>27</sup> The above expressions have been derived for  $I_b=0$ . For nonzero bias current we expect Eq. (3) to be valid, with  $f_{\text{pl},0}$  now given by  $f_{\text{pl}}(H_{\perp})$ .

Data are shown in Fig. 10. In zero magnetic field the conversion again rose until  $I_{cn}^*$  was reached. The mixing signals shifted in different magnetic fields according to the decrease of the critical currents thus confirming the shift of the resonance frequency. Unfortunately, it was very tedious to measure at higher fields due to strong pinning. Therefore, we concentrate on experiments with parallel magnetic field.

#### B. Magnetic field parallel to the $\text{CuO}_2$ layers

Applying a magnetic field with small tilt angles between the  $\text{CuO}_2$  planes and field orientation we were able to decrease the plasma frequency significantly. In Fig. 11 we plot the conversion intensity measured on the superconducting branch as function of bias current at various fields. At weak magnetic field we only detected the uprise close to  $I_{cn}^*$ . With increasing field  $H_{\parallel}$  a conversion peak developed just below  $I_{cn}^*$ . Further rising  $H_{\parallel}$  shifted the conversion peak towards lower bias currents. This can be explained by the decrease of the plasma frequency due to the decrease of  $j_c$  in a magnetic field. As a consequence, less bias current had to be applied in order to match the plasma resonance to the LO frequency. Figure 12 shows the peak current values as a function of

magnetic field  $H_{\parallel}$ . The peak currents decreased as  $H_{\parallel}^{-\nu}$ . For our samples we derive  $0.57 < \nu < 0.86$ .

From this behavior we were able to determine the Josephson plasma frequency. Assuming that Eq. (3) is still valid we write:

$$f_{\text{pl}}(H_{\parallel}, I_b = I_{\text{peak}}) = f_{\text{LO}} = f_{\text{pl}}(H_{\parallel}, 0) \sqrt[4]{1 - \left(\frac{I_{\text{peak}}(H_{\parallel})}{I_c(H_{\parallel})}\right)^2}, \quad (14)$$

where we identified  $f_{\text{pl}} = f_{\text{LO}}$  for  $I_b = I_{\text{peak}}$ . Now, the Josephson plasma resonance can be regarded as a function of magnetic field only. To estimate the value of the Josephson plasma resonance at zero bias and zero magnetic field we have to insert the dependence of the plasma resonance on  $H_{\parallel}$ . We approximate the magnetic field dependence of  $f_{\text{pl}}(H_{\parallel}, 0)$  by the assumption that it will change via  $I_c(H_{\parallel})$  according to Eq. (2).

We thus get

$$f_{\text{pl},0} \approx \frac{f_{\text{LO}}}{\sqrt[4]{\frac{I_c(H_{\parallel})}{I_c(0)} \sqrt[4]{1 - \left(\frac{I_{\text{peak}}(H_{\parallel})}{I_c(H_{\parallel})}\right)^2}}} \quad (15)$$

and could estimate the plasma frequency at zero magnetic field and zero bias. Figure 13 shows the derived plasma frequencies as function of the measured critical current densities at zero field. Depending on  $j_c$  we obtain  $f_{\text{pl},0}$  ranging between 105 GHz and 220 GHz. Fitting these results with Eq. (2) with the dielectric constant  $\epsilon_r$  being the fitting parameter we obtain  $\epsilon_r = 3.5$ .

## VII. CONCLUSIONS

We realized a heterodyne mixer with mesas patterned on top of  $\text{Bi}_2\text{Sr}_2\text{CaCu}_2\text{O}_{8+y}$  single crystals. The mixer saturates at rather low LO powers. The observed mixing behavior can be well explained by interactions between the external microwave signals and the collective Josephson plasma resonance of a stack of intrinsic Josephson junctions. The intensity of the IF signal is independent of the number of junctions when only a few junctions are in the resistive state. From that we conclude that it is the *collective* Josephson plasma resonance causing the mixing process. From the mixing signals in magnetic fields parallel to the layers we were able to extrapolate the Josephson plasma frequencies at zero field and zero bias current. Depending on  $j_c$  they ranged between 105 GHz and 220 GHz.

## ACKNOWLEDGMENTS

The authors would like to thank L. N. Bulaevskii, K. Schlenga, and O. Waldmann for valuable discussions and H. L. Johnson and S. Schmitt for providing and preparing samples. H. J. Hartfuss and K. H. Gundlach provided the W-band mixer block. Financial support by Bayerische Forschungsförderung via the FORSUPRA consortium is gratefully acknowledged.

- <sup>1</sup>S. Beuven, O. Harnack, L. Amatuni, H. Kohlstedt, and M. Darula, *IEEE Trans. Appl. Supercond.* **7**, 2591 (1997).
- <sup>2</sup>B. D. Josephson, in *Quantum Fluids*, edited by D. F. Brewer (North-Holland, Amsterdam, 1966).
- <sup>3</sup>A. I. Dahm, A. Denenstien, T. F. Finnegan, D. N. Langenberg, and D. J. Scalapino, *Phys. Rev. Lett.* **20**, 859 (1968).
- <sup>4</sup>R. Kleiner, F. Steinmeyer, G. Kunkel, and P. Müller, *Phys. Rev. Lett.* **68**, 2394 (1992); R. Kleiner and P. Müller, *Phys. Rev. B* **49**, 1327 (1994).
- <sup>5</sup>M. Tachiki, T. Koyama, and S. Takahashi, *Phys. Rev. B* **50**, 7065 (1994).
- <sup>6</sup>O. K. C. Tsui, N. P. Ong, Y. Matsuda, Y. F. Yan, and J. B. Peterson, *Phys. Rev. Lett.* **73**, 724 (1994).
- <sup>7</sup>Y. Matsuda, M. B. Gaifullin, K. Kumagai, K. Kadowaki, and T. Mochiku, *Phys. Rev. Lett.* **75**, 4512 (1995).
- <sup>8</sup>O. K. C. Tsui, N. P. Ong, and J. B. Peterson, *Phys. Rev. Lett.* **76**, 819 (1996).
- <sup>9</sup>A. Yurgens, D. Winkler, Y. M. Zhang, N. Zavaritsky, and T. Claeson, *Physica C* **235–240**, 3269 (1995).
- <sup>10</sup>A. Barone and G. Paternò, *Physics and Applications of the Josephson Effect* (John Wiley, New York, 1982).
- <sup>11</sup>N. F. Pedersen, M. R. Samuelsen, and K. Saermark, *J. Appl. Phys.* **44**, 5120 (1973).
- <sup>12</sup>M. J. Feldman, P. T. Parrish, and R. Y. Chiao, *J. Appl. Phys.* **46**, 4031 (1975).
- <sup>13</sup>J. M. Manley and H. E. Rowe, *Proc. IRE* **44**, 904 (1956).
- <sup>14</sup>G. Hechtfisher, R. Kleiner, K. Schlenga, W. Walkenhorst, P. Müller, and H. L. Johnson, *Phys. Rev. B* **55**, 14 638 (1997).
- <sup>15</sup>H. Shibata and T. Yamada (unpublished).
- <sup>16</sup>L. N. Bulaevskii, D. Dominguez, M. P. Maley, A. R. Bishop, O. K. C. Tsui, and N. P. Ong, *Phys. Rev. B* **54**, 7521 (1996).
- <sup>17</sup>Provided by H. J. Hartfuss, MPI/IPP Garching and K. H. Gundlach, IRAM Grenoble.
- <sup>18</sup>W. Walkenhorst, G. Hechtfisher, M. Mößle, K. Schlenga, S. Schlötzer, S. Schmitt, R. Kleiner, and P. Müller (unpublished).
- <sup>19</sup>G. Hechtfisher, W. Walkenhorst, G. Kunkel, K. Schlenga, R. Kleiner, P. Müller, and H. L. Johnson, *IEEE Trans. Appl. Supercond.* **7**, 2723 (1997).
- <sup>20</sup>H. L. Johnson, CSIRO, Lindfield, Australia.
- <sup>21</sup>G. J. Dolan, T. G. Phillips, and D. P. Woody, *Appl. Phys. Lett.* **34**, 347 (1979).
- <sup>22</sup>M. R. Barber, *IEEE Trans. Microwave Theory Tech.* **15**, 629 (1967).
- <sup>23</sup>J. R. Tucker and M. J. Feldman, *Rev. Mod. Phys.* **57**, 1055 (1985).
- <sup>24</sup>B. A. Huberman, J. P. Crutchfield, and N. H. Packard, *Appl. Phys. Lett.* **37**, 750 (1980).
- <sup>25</sup>R. Kleiner, P. Müller, H. Kohlstedt, N. F. Pedersen, and S. Sakai, *Phys. Rev. B* **50**, 3942 (1994).
- <sup>26</sup>L. N. Bulaevskii, D. Dominguez, M. P. Maley, A. R. Bishop, and B. I. Ivlev, *Phys. Rev. B* **53**, 14 601 (1996).
- <sup>27</sup>L. N. Bulaevskii, V. L. Pokrovsky, and M. P. Maley, *Phys. Rev. Lett.* **76**, 1719 (1996).
- <sup>28</sup>L. N. Bulaevskii, D. Dominguez, M. P. Maley, and A. R. Bishop, *Phys. Rev. B* **55**, 8482 (1997).
- <sup>29</sup>Y. Matsuda, M. B. Gaifullin, K. Kumagai, K. Kadowaki, T. Mochiku, and K. Hirata, *Phys. Rev. B* **55**, R8685 (1997).